NeuroImage 114 (2015) 217–225

Contents lists available at ScienceDirect

NeuroImage

journal homepage: www.elsevier.com/locate/ynimg

Network-level reorganisation of functional connectivity following arm amputation

Tamar R. Makin [a,*], Nicola Filippini [a,b], Eugene P. Duff [a], David Henderson Slater [a,c], Irene Tracey [a,d], Heidi Johansen-Berg [a]

[a] FMRIB Centre, Nuffield Department of Clinical Neurosciences, University of Oxford, Oxford OX3 9DU, UK
[b] Department of Psychiatry, Warneford Hospital, Oxford OX3 7JX, UK
[c] Oxford Centre for Enablement, Nuffield Orthopaedic Centre, Oxford OX3 7HE, UK
[d] Nuffield Division of Anaesthetics, Nuffield Department of Clinical Neuroscience, University of Oxford, Oxford OX3 9DU, UK

ARTICLE INFO

Article history:
Received 20 October 2014
Accepted 26 February 2015
Available online 14 March 2015

Keywords:
Neuroimaging
Deprivation
Plasticity
Resting state networks
Somatosensory
Motor

ABSTRACT

One of the most striking demonstrations of plasticity in the adult human brain follows peripheral injury, such as amputation. In the primary sensorimotor cortex, arm amputation results in massive local remapping of the missing hands' cortical territory. However, little is known about the consequences of sensorimotor deprivation on global brain organisation. Here, we used resting-state fMRI to identify large-scale reorganisation beyond the primary sensorimotor cortex in arm amputees, compared with two-handed controls. Specifically, we characterised changes in functional connectivity between the cortical territory of the missing hand in the primary sensorimotor cortex ('missing hand cortex') and two networks of interest: the sensorimotor network, which is typically strongly associated with the hand cortex, and the default mode network (DMN), which is normally dissociated from it. Functional connectivity values between the missing hand cortex and the sensorimotor network were reduced in amputees, and connectivity was weaker in individuals amputated for longer periods. Lower levels of functional coupling between the missing hand cortex and the sensorimotor network were also associated with emerged coupling of this cortex with the DMN. Our results demonstrate that plasticity following arm amputation is not restricted to local remapping occurring within the sensorimotor homunculus of the missing hand but rather produces a cascade of cortical reorganisation at a network-level scale. These findings may provide a new framework for understanding how local deprivation following amputation could elicit complex perceptual experiences of phantom sensations, such as phantom pain.

Introduction

Our brain's ability to reorganise itself throughout life is a key mechanism that enables adjustment to novel situations, as well as compensation for injury. Arm amputation is a powerful driver of brain plasticity, as it combines sensorimotor deprivation with profound behavioural changes, encompassing both acquisition of compensatory motor skills and coping with a chronic pain condition (phantom limb pain which is a common consequence of arm amputation Weeks et al., 2010). Despite these global consequences on perception and action, amputation has been primarily used as a model for studying local plasticity, consequential to focal input loss.

In the primary somatosensory cortex (SI), sensory deprivation leads to recruitment of the input-deprived cortex by neighbouring cortical representations, resulting in massive structural (Florence et al., 1998) and functional (Pons et al., 1991) areal cortical reorganisation. Most notably, studies in monkeys show remapping of the somatosensory homunculus, such that the area originally devoted to the missing hand (here after 'missing hand cortex') now becomes responsive to inputs applied to the monkey's lower face (Florence et al., 1998; Jain et al., 2008; Pons et al., 1991). As in animal research, human research in amputees has largely focused on plasticity in the primary sensorimotor cortex of the hemisphere contralateral to the amputation. The remapping of the lower face representation, associated with sensory deprivation, has widely been considered to reflect maladaptive plasticity, as it has been shown to correlate with phantom limb pain (Flor et al., 1995, 2006; Lotze et al., 2001). Yet, the mechanisms linking local remapping with complex phenomenology such as chronic phantom pain, as well as other sensations arising from the "phantom hand" are still largely unknown.

Since the primary sensorimotor areas are interconnected with higher-order sensorimotor areas (e.g. premotor cortex, Brodmann area 6 (Yeo et al., 2011)), as well as with association cortex (e.g., the superior parietal lobe (Markov et al., 2013; Rizzolatti and Matelli, 2003)), local reorganisation is likely to cascade changes in connectivity both within and beyond the sensorimotor system. Indeed, visual

* Corresponding author at: FMRIB Centre, John Radcliffe Hospital, Oxford OX3 9DU, UK.
E-mail address: tamar.makin@ndcn.ox.ac.uk (T.R. Makin).

http://dx.doi.org/10.1016/j.neuroimage.2015.02.067

information of the hand is integral for motor processing during action in the healthy brain (Makin et al., 2014). We have previously shown that amputation of the hand leads to shifts in visuospatial perception (Makin et al., 2010), as well reductions in visuomotor object affordances (Wilf et al., 2013), demonstrating functional consequences to amputation that had not been considered before and that may result from reorganisation beyond the sensorimotor cortex.

An increasingly popular approach to studying long-range interactions in both healthy (Smith et al., 2009, 2012; Yeo et al., 2011) and clinical populations (Collignon et al., 2013; Napadow et al., 2010; Rocca et al., 2014) is by measuring resting state functional connectivity. Functional connectivity is a measure of spatiotemporal synchrony of fMRI Blood-Oxygenation-Level-Dependent (BOLD) signal between anatomically distinct brain regions (Friston et al., 1993), and it represents the degree of functional de/coupling between dissociated brain areas. While participants are at rest, spontaneous fluctuations in the BOLD signal can be used to infer functional connectivity between intrinsically correlated brain regions (Biswal et al., 1995). Since functional networks have distinct temporal characteristics, separate networks can be identified from a single time-series of resting fMRI data (Beckmann et al., 2005). Moreover, unlike other functional methods that utilise sensorimotor tasks to characterise activation in the deprived cortex, the resting state approach avoids potential confounds of compensatory activation and therefore allows a new exploration of the consequences of amputation.

We have recently shown that amputees suffering from chronic phantom pain show maintained function and structure in the missing hand cortex, as well as reduced functional connectivity between the two hand areas as measured using resting-state fMRI (Makin et al., 2013b). We speculated that this reduced connectivity between the hand areas reflected functional isolation of the phantom cortex from the sensorimotor system. Here, we take this idea further by exploring global network-level changes in functional connectivity within and beyond the sensorimotor system following amputation in adults, using resting state functional connectivity.

Since phantom sensations are manifested in an incorporeal bodypart, they can be regarded as internal modes of sensation (i.e. mostly decoupled from events in the external environment). We therefore predicted that the missing hand cortex, which is engaged with phantom sensations, should become dissociated from its original network (sensorimotor), and associated with other brain networks that are involved with the representation of internalised sensations. In particular, the default mode network (DMN) is usually not active while participants are engaged with their environment, but is rather activated by internal modes of sensation (Buckner et al., 2008). The aim of the present study was therefore to characterise large scale intra-network (within the sensorimotor network) and inter-network (between the sensorimotor network and the DMN) plasticity following arm amputation, and its relationship with phenomenology of phantom limb sensations.

Methods

Participants

18 individuals with acquired unilateral upper limb amputation (mean age ± s.e.m. = 46 ± 3, 6 with absent right hand, see Table 1) were recruited through the Oxford Centre for Enablement and Opcare. 22 healthy controls, matched for handedness (7 left-hand dominant), age (41 ± 3) and education were also recruited (see Table S1). Handedness was defined in the amputees based on the hand currently used for lateralised tasks, such as writing (i.e. the intact hand), regardless of handedness prior to the injury. Note that the average time since amputation for the subset of 5 amputees who lost their dominant hand (and were therefore forced to rely on their originally non-dominant hand) was 27 years (Table 1). Procedures were in accordance with NHS national research ethics service approval (10/H0707/29), and written informed consent was obtained. The participants were studied intensively using a range of neuroimaging and behavioural tests and some of these data have been used to address distinct questions previously (Makin et al., 2013a, 2013b). Data from one control were discarded from the resting state analyses, due to excessive head movements (>3 mm).

Phantom sensation rating

Amputees rated the frequencies of phantom/stump pain and non-painful phantom sensations, as experienced within the last year, as well as intensity of worst pain experienced during the last week (or in a typical week involving phantom/stump sensations). 'Pain magnitude' was calculated by dividing pain intensity (0: 'no pain'–10: 'worst pain imaginable') by frequency (1–'all the time', 2 –'daily', 3–'weekly', 4–'several times per month' and 5–'once or less per month'). This measure therefore reflects the chronic aspect of the pain as it combines both frequency and intensity, as used previously (Draganski et al., 2006; Makin et al., 2013b). An analogous measure was obtained for vividness of non-painful phantom sensations. Ratings of 'averaged phantom pain' (as experienced in the last week, or in a typical week involving phantom

Table 1
Demographic and clinical details of the amputees, and individual imaging values.

	Age	Age at amp.	Amp. level	Side/dominant	Phantom sensation Mag./scan	Phantom pain Mag./scan	Cause of amp	FC with SMN	FC with DMN
A01	43	38	4	L/R	10/10	7/8	Trauma	9.21	4.15
A02	42	22	4	R/L	1.74/5	2.5/0	Nerve I*	9.22	−.31
A03	21	18	4	R/L	8/9	3.33/0	Trauma	12.55	.29
A04	46	37	2	L/R	3/2	2/0	Nerve I*	10.97	−.42
A05	48	20	1	R/R	10/7	4.5/1	Trauma	6.68	.37
A06	58	11	2	R/R	1.2/6	1.75/0	Trauma	6.56	2.40
A07	31	2	2	L/R	0/0	0/0	Trauma	6.99	1.66
A08	54	20	5	L/L	10/10	4/4	Trauma	7.17	1.48
A09	47	45	2	L/L	9/9	8/4	Tumour	15.59	.22
A10	60	34	2	R/R	8/6	1/0	Trauma	9.03	-.27
A11	51	35	4	L/R	5/2	1.75/1	Infection	7.29	2.66
A12	47	19	2	L/R	4.5/6	4.5/4	Trauma*	5.66	3.28
A13	57	48	4	R/L	3.5/7	1.5/6	Infection	7.15	2.33
A14	56	40	2	L/R	8/10	1.75/0	Trauma	9.93	1.02
A15	22	18	5	L/R	10/10	1/0	Trauma	8.19	−1.30
A16	43	33	4	L/R	2.67/4	2.33/0	Trauma	7.70	.23
A17	50	28	4	L/R	5/2	3/0	Trauma	9.47	2.50
A18	52	45	4	L/R	1.33/0	0/0	Trauma	13.07	.22

Amp. = amputation; amputation levels: 1 = wrist, 2 = below elbow, 3 = through elbow, 4 = above elbow, 5 = through shoulder; side = side of amputation; dominant = hand dominance prior to amputation (based on self report) – L = left, R = right; Mag. = magnitude; scan = score of pain intensity/phantom sensation vividness on scanning day; nerve I = nerve injury; * indicates potential partial spinal damage; FC = functional connectivity with the missing hand cortex; SMN = sensorimotor network; DMN = default mode network.

pain) as well as current pain/vividness (described here as 'scan phantom pain/sensation') were also obtained before the scanning session, using the 0–10 pain scale described above.

Scanning procedures

The MRI measurements were obtained using a 3 Tesla Verio scanner (Siemens, Erlangen, Germany) with a 32-channel head coil. Anatomical data was acquired using a T1-weighted magnetization prepared rapid acquisition gradient echo sequence (MPRAGE) with the parameters: TR = 2040 ms; TE = 4.7 ms; flip angle = 8°, voxel size = 1 mm isotropic resolution. Functional data based on the BOLD signal were acquired using a multiple gradient echo-planar T2*-weighted pulse sequence, with the parameters: TR = 2410 ms, TE = 30 ms, flip angle = 90°, imaging matrix = 64 × 64, FOV = 192 mm axial slices. 44 slices with slice thickness of 3 mm and no gap were oriented in the oblique axial plane, covering the whole cortex, with partial coverage of the cerebellum. A total of 128 volumes were collected, during which participants were asked to lie still in a dimmed room with their eyes open. They were explicitly asked not to move any body-parts.

Preprocessing

All imaging data were processed using FSL 5.1 (www.fmrib.ox.ac.uk/fsl). Since our amputee group consisted of both left and right hand amputees, the hemispheres were standardised based on laterality with respect to the missing hand (Bogdanov et al., 2012; Diers et al., 2010; Foell et al., 2013; Lotze et al., 2001; MacIver et al., 2008; Raffin et al., 2012). This procedure is regularly exercised in functional connectivity studies involving lateralised populations (e.g. (Douaud et al., 2011; Park et al., 2011)). Data collected for individuals with absent right hands (6 amputees), were therefore mirror reversed across the mid-sagittal plane prior to all analyses so that the hemisphere corresponding to the missing hand was consistently aligned. To ensure that the reversal procedure didn't introduce any biases across the two groups, data collected for left-hand dominant controls (n = 7), consisting of the same proportion as right-hand amputees (33%), was also mirror reversed, in order to account for potential biases stemming from this procedure. See the Supplementary section for further analysis addressing the potential confound of network asymmetry.

Functional data was analysed using FMRIB's expert analysis tool (FEAT, version 5.98). The following pre-statistics processing was applied to each individual run: a) motion correction using FMRIB's Linear Image Registration Tool (MCFLIRT); absolute head motion parameters were compared between groups, with no significant differences ($p > 0.34$); b) brain-extraction using BET; c) mean-based intensity normalization; d) high pass temporal filtering of 150 s (0.007 Hz); e) spatial smoothing using a Gaussian kernel of 6 mm FWHM (full width at half maximum). No low-pass filtering was applied, in accordance with recent reports showing that resting state networks show temporal coherences across a wide frequency spectrum, suggesting a broadband process (Niazy et al., 2011). Time-series statistical analysis was carried out using FILM (FMRIB's Improved Linear Model) with local autocorrelation correction. Functional data was aligned to structural images (within-subject) initially using linear registration (FMRIB's Linear Image Registration Tool, FLIRT), then optimized using Boundary-Based Registration (Greve and Fischl, 2009), as implemented in FEAT. Structural images were transformed to standard MNI space using a non-linear registration tool (FNIRT), and the resulting warp fields applied to the functional statistical summary images.

Independent component analysis

Data were further analysed using MELODIC (Multivariate Exploratory Linear Optimized Decomposition into Independent Components, part of FSL http://www.fmrib.ox.ac.uk/fsl/melodic/). Individual scans were temporally concatenated across both groups to create a single 4D dataset. Preliminary independent component analysis (ICA) using Bayesian dimensionality estimation resulted in 16 independent components which didn't capture the full set of canonical networks as previously reported (Beckmann et al., 2005). To allow a comparable analysis to previous and future studies, we increased the dimensionality to 25 components (as previously implemented by Filippini et al., 2009, 2012). Each of the resulting components was compared with a set of previously defined maps (Filippini et al., 2009) using whole-brain spatial correlation to identify the 8 canonical networks (Beckmann et al., 2005).

For presentation purposes, statistical parametric activation maps showing each of the networks were projected on an averaged inflated surface of a cortex, using Connectome Workbench (http://www.humanconnectome.org/software/connectome-workbench.html).

Whole brain analysis of functional connectivity

A voxel-based general linear model (GLM) was carried out as implemented in FSL. To compute voxel-based functional connectivity maps in individual participants with the group ICA-based resting state networks, we used the dual regression approach (Filippini et al., 2009): The main regressor of interest was the averaged time course underlying the IC of interest, with individual voxels weighted based on their contribution to the group IC. The weighted time-courses of all other ICs were also calculated within each individual participant, using the same procedure, and included as regressors of no interest, in a voxel-wise first-level GLM. The output values of this analysis are voxel-wise beta values, representing the strength of connectivity of this voxel to the components of interest, after accounting for partial contribution of all other ICs. This analysis was repeated twice for each participant, to identify the strength of connectivity between individual voxels and the two group components of interest (sensorimotor, Figs. 1A–B; DMN, Figs. 2A–B). In addition, a similar analysis was further carried to explore changes in connectivity with the pain-related insular-operculum network (Fig. S1A), as well as a control component (executive-control, Fig. S2A).

Since our study was designed to address changes in connectivity specifically relating to the territory of the missing hand, we focused on a region of interest (ROI) analysis. To identify further regions where the networks of interest differed in their strength across groups, whole-brain group comparisons were also performed for each of the two networks of interest, using permutation test (as applied in FSL's randomise) and threshold-free cluster estimate.

ROI analysis of functional connectivity

Individual time-series from the 'missing' hand area (or the nondominant hand area in controls) were extracted using a group ROI, which we previously used to characterise the "deprived cortex" (as fully described in Makin et al., 2013a, 2013b). In brief, this ROI was based on the averaged activation for the same populations of amputees and controls, during a task-based block-design fMRI scan. During this scan, participants were requested to perform simple hand movements with each of their hands (including the phantom hand for amputees, see Makin et al., 2013b for full details). Activation resulting from each of the hand conditions was contrasted with activation during bilateral feet movements. Activation maps were flipped on the horizontal plane for amputees with a missing right hand and control participants who were left-hand dominant. The resulting contrast maps were averaged across amputees and controls, such that the phantom-hand selective maps were averaged with controls' nondominant hand maps, and amputees' intact hand selective maps were averaged with controls dominant hand maps. The resulting group map was thresholded at $Z > 7$. The resulting clusters centred on the anatomical hand knob of the central sulcus contralateral to the missing/nondominant hand and the intact/dominant hand were used as group ROIs.

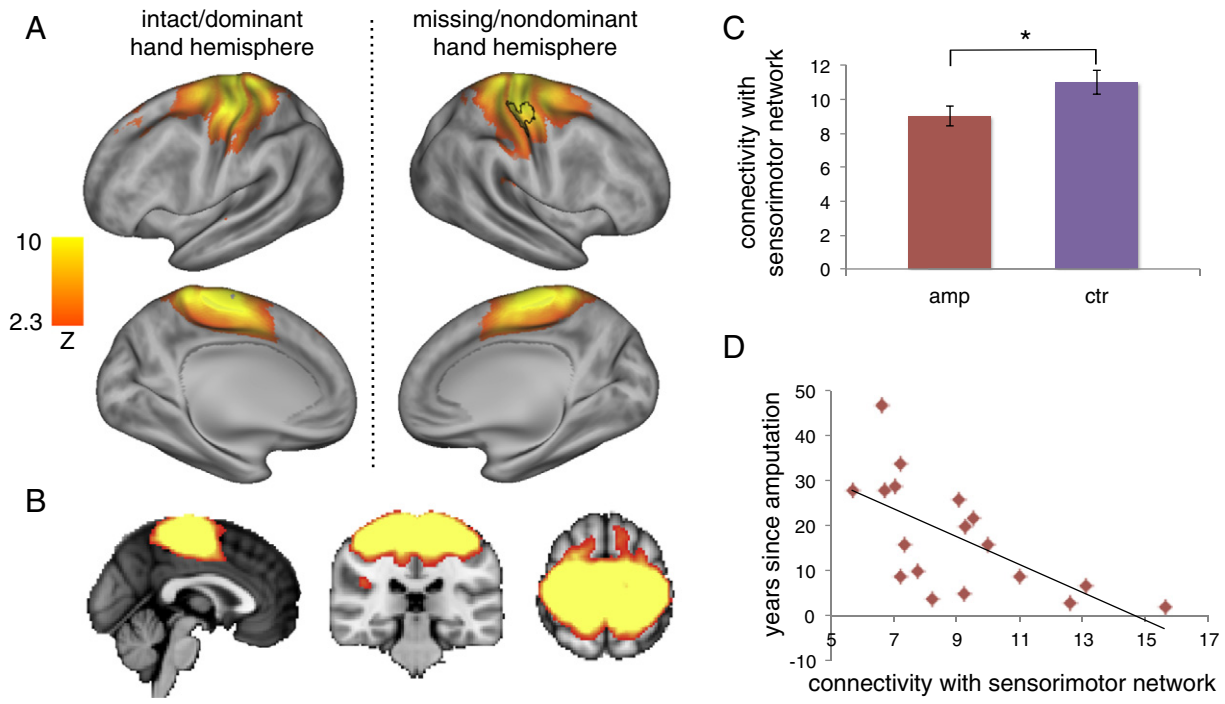

Fig. 1. Decreased functional connectivity between the missing hand ROI and the sensorimotor network in amputees. (A) The ICA component corresponding to the sensorimotor network. The thresholded network (red to yellow clusters) and the missing hand region of interest (ROI) (black outline, $z > 7$) are projected on a cortical surface of an averaged brain. (B) The same network is overlaid on a standard MNI template brain, shown in sagittal, coronal, and axial views (left to right). (C) Mean voxel-wise connectivity values between the missing hand ROI and the sensorimotor network in amputees (amp, red) and controls (ctr, purple). The error bars show s.e.m. in the two groups. (D) Within the amputee group, connectivity strength between the missing hand ROI and sensorimotor network was associated with time since amputation. Intact/dominant hand hemisphere is the hemisphere contralateral to the intact hand in amputees and dominant hand in controls. Missing/nondominant hand hemisphere is the hemisphere contralateral to the missing hand in amputees and the dominant hand in controls. The regression line is plotted for visualisation purposes only, as it doesn't denote the ranked correlation between the two measurements that was used for statistical inference.

The area resulting from the phantom/nondominant hand contrast, shown as a black contour in Figs. 1A and 2A, therefore reflects the estimated cortical territory of the missing hand in amputees (and the nondominant hand in controls). This ROI was transformed to individual space and GLM parameter estimates from the individual statistical parametric maps (resulting from the dual regression analysis) were

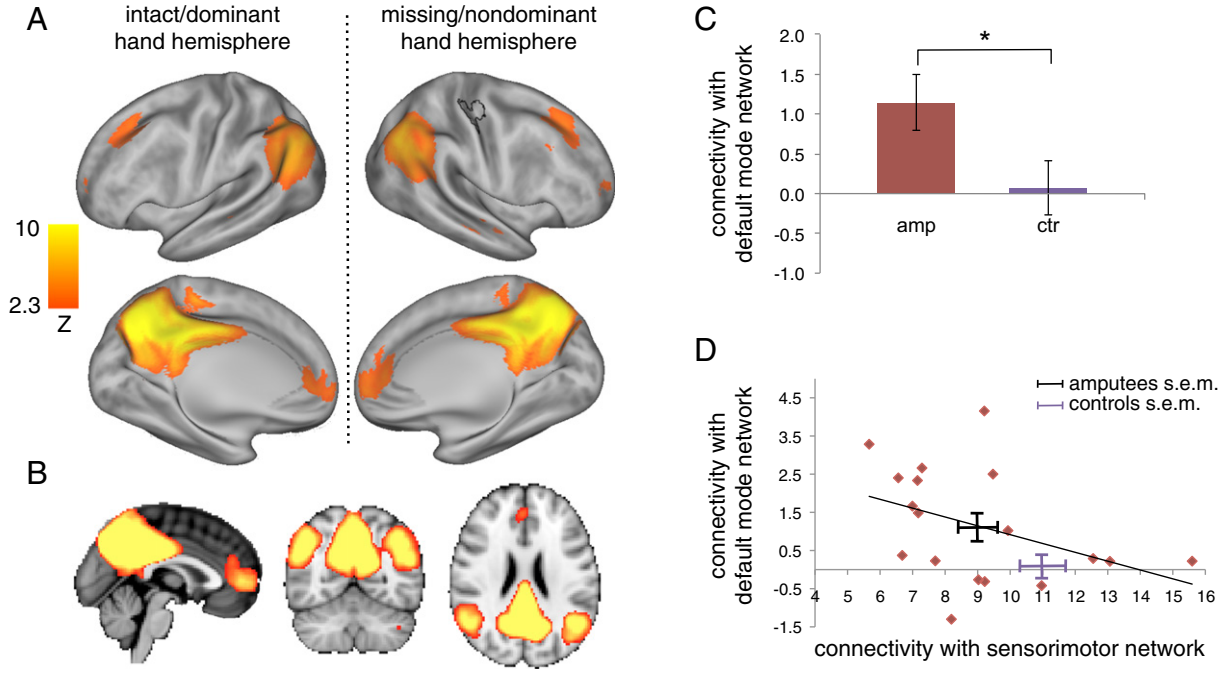

Fig. 2. Increased functional connectivity between the missing hand ROI and the default mode network in amputees. (A–B) The ICA component corresponding to the default mode network (DMN) is displayed as in Fig. 1. (C) Mean voxel-wise connectivity values between the missing hand region of interest (ROI) and the DMN are shown as in Fig. 1. (D) Connectivity strength between the missing hand ROI and the two networks (sensorimotor and DMN) in individual amputees. The crosses indicate the mean ± s.e.m. for connectivity between the missing hand's territory and each of the two main networks of interest (sensorimotor and DMN) in the controls (purple) and amputee (black) groups. Other annotations are as in Fig. 1.

extracted for each of the 2 networks of interest (sensorimotor and DMN), as well as two additional control networks (insular-operculum network, Fig. S1 and executive control network, Fig. S2). An intact hand ROI, based on intact/dominant hand movements in the two groups (Makin et al., 2013b) was used for control purposes. For each participant, data was extracted from each of the ROIs and beta values were averaged across voxels within each ROI. The resulting measurement reflects the level of connectivity between the ROI and the network of interest.

Statistical comparisons of ROI analysis

Between-group and repeated measure effects (between the hemispheres contralateral and ipsilateral to the missing hand) were statistically compared initially using mixed model ANOVAs. The main parameters were: ROI (intact, missing); network (sensorimotor, DMN); and group (amputees, controls). In accordance with the best statistical practice (Nieuwenhuis et al., 2011), a 3-way ANOVA was initially conducted. Significant interactions were subsequently interpreted using 2-way ANOVAs. Effect sources, as driven by our research question, were finally interrogated using two orthogonal planned comparisons. Specifically, the prediction that connectivity between the missing hand ROI and between the two networks of interest is altered in amputees was tested using (uncorrected) independent-samples 2-tailed tests. Comparisons against zero, used to further interpret the planned comparison relating to connectivity with the DMN, were carried out using a 2-tailed one-sample t-test. Correlations were evaluated using a 2-tailed Spearman test, which is less susceptible to exaggerated effects due to outliers. To test whether these correlations were stronger in amputees versus controls we transformed the rho values to z values using Fisher's transformation and compared their strength using a 1-tailed test. Statistical analysis was carried with SPSS version 18.

Seed analysis

To calculate seed voxel-based functional connectivity maps, individual time-series were extracted from the missing hand group ROI. The ROI was transformed to individual space, and used as an individualised 'seed' to model the activation time-course in a first level FEAT analysis. In addition, to account for potential contributions of physiological noise, time-series extracted from group white matter and cerebrospinal fluid masks were used as nuisance regressors, along with head motion parameters.

Group level analysis of spatial maps was carried out using FMRIB's Local Analysis of Mixed Effects (FLAME). The cross-subject general linear model (GLM) included the two groups. Z (Gaussianised TF) statistic images were thresholded using clusters determined by $Z > 2$ and a family-wise-error corrected cluster significance threshold of $p < 0.05$ was applied to the suprathreshold clusters. For presentation purposes, statistical parametric activation maps were projected on an averaged inflated surface cortex, using Connectome Workbench (http://www.humanconnectome.org/software/connectome-workbench.html).

To investigate the direction of connectivity changes underlying these group level seed-based functional connectivity maps, we calculated the average beta values underlying the (unthresholded) connectivity maps in individual participants. We took an analogous approach to that used in the dual regression analysis: The beta values in each voxel in each individual participant's seed-based functional connectivity map, representing the strength of connectivity between this voxel and the missing/nondominant hand ROI, were weighted based on their corresponding z statistics in the unthresholded group contrast map and then averaged for each participant. The resulting average therefore indicates the level of connectivity between the seed area and the group map in each individual.

Correlations with clinical and demographic details

In order to estimate the relationship between functional connectivity and clinical details relating to the amputation, we first ran a series of bivariate correlations between subject-specific connectivity levels (between the missing hand ROI and the two networks of interest, as well as the insular-operculum network) and the clinical ratings, using a spearman rho test. Results relating to each network were corrected for multiple comparisons using the Bonferroni approach (see Table S2) for 8 comparisons, based on the following variables: (a) Phantom sensation magnitude (a measurement of chronic non-painful phantom sensations, taking under consideration both intensity and frequency); (b) nonpainful phantom sensations vividness, as experienced during the scanning session; (c) phantom pain magnitude (homologous to phantom sensation magnitude); (d) phantom pain intensity, as experienced during the scanning session. (e) Averaged phantom pain intensity, during the course of a typical week; (f) stump pain magnitude; (g) time since amputation; (h) amputation level. We also tested for a correlation between connectivity levels and the spectral power underlying the missing hand ROI. We next inserted all the clinical variables that are suitable for parametric testing (i.e. normally distributed, as determined by the Shapiro–Wilk test) as independent variables in a backward linear regression model. These parameters were: (a) Phantom sensation magnitude; (b) nonpainful phantom sensations vividness; (c) phantom pain magnitude; (d) averaged phantom pain intensity; (d) time since amputation. For the DMN, connectivity between the missing hand cortex and the sensorimotor network was also included. The dependent variable was strength of connectivity of either the DMN or the sensorimotor network with the missing hand ROI.

Results

Inter-network plasticity, dual regression analysis

To examine how sensory deprivation following arm amputation affects large scale functional architecture, we applied an ICA to resting-state scans (Beckmann et al., 2005). This approach has been shown to capture a large repertoire of functional networks utilised by the brain in action (Smith et al., 2009). Of 8 components, corresponding to the canonical functional networks (Beckmann et al., 2005), we were interested in studying connectivity differences in the sensorimotor network (Figs. 1A–B), which spatially overlaps with the hand ROIs; and the DMN (Figs. 2A–B), spanning the paracingulate gyrus; posterior cingulate; precuneus; and the angular gyrus (Greicius et al., 2003; Raichle et al., 2001). A dual regression approach was carried out to estimate the level of voxel-wise connectivity within each of the bilateral hand ROIs to each of the networks of interest, while regressing out partial contributions resulting from all other ICA components. This approach was designed to regress out any common sources of variance to provide a measure of the unique temporal relationship between the target voxels (hand ROIs) and the functional network of interest (Filippini et al., 2009). The voxel-wise beta values resulting from this analysis were extracted from two main ROIs for each individual participant, as a measurement of connectivity strength between each of the ROIs and each of the networks of interest. When conducting a whole-brain contrast, no group differences were observed in the two networks of interest, suggesting that the networks may not be different between the two groups.

We hypothesised that amputation should induce specific effects on the missing hand cortex (but not the intact hand cortex), and that the direction of these effects should vary between networks. To test this prediction, we conducted a series of mixed-model ANOVAs, using the parameters: ROI (intact and missing hand areas); network (sensorimotor and DMN); and, group (amputees and controls). This approach revealed a significant 3-way interaction ($F_{(1,37)} = 6.54$, $p = 0.015$), supporting our prediction that connectivity to the missing hand

territory is changed differently across hemispheres and networks in amputees, compared with controls.

To determine whether the interaction was driven by changed connectivity with respect to the missing hand, and not the intact hand, the analysis was followed up using separate ANOVAs for each hand ROI, using the parameters: network (sensorimotor, DMN) and group (amputees, controls). As predicted, a significant interaction between group and network was found for the missing hand ROI ($F_{(1,37)} = 8.41$, $p = 0.006$), but not for the intact hand ROI ($F_{(1,37)} = 0.04$, $p = 0.836$). Together, these analyses suggest that functional coupling patterns in the missing hand ROI vary between groups and networks, specifically.

Further analyses focused on functional connectivity levels within the missing hand ROI for each of the networks of interest, using two between-group planned comparisons. This was carried out in order to verify that amputation results in different connectivity levels between the missing hand ROI and each of the networks of interest, and to identify the direction of connectivity changes between groups. For the sensorimotor network, we identified significantly decreased connectivity in amputees compared with controls ($t_{(37)} = -2.05$, $p = 0.048$; Fig. 1C). This means that connectivity is reduced between the missing hand ROI and its typical network of origin (sensorimotor) in amputees. By contrast, for the DMN, connectivity was significantly greater in amputees than in controls ($t_{(37)} = 2.18$, $p = 0.035$, Fig. 2C). While in controls the missing hand ROI was decoupled from the DMN (i.e., connectivity value is close to zero, Fig. 2C), in the amputee group the connectivity between the missing hand ROI and the DMN was significantly greater than zero ($t_{(17)} = 3.26$, $p = 0.005$). This means that connectivity is increased between the missing hand ROI and the (typically dissociated) DMN in amputees. Importantly, within the amputee group, connectivity levels between the missing hand ROI and the DMN were negatively correlated with connectivity with the sensorimotor network: participants showing greater decoupling between the missing hand cortex and the sensorimotor network also showed increased coupling with the DMN ($\rho_{(16)} = -0.488$, $p = 0.040$; Fig. 2D).

Control analyses

To ensure that these effects (and the decoupling from the sensorimotor network in particular) were not caused by reduced overall levels of activity in the missing hand cortex (i.e. a change in signal-to-noise ratio; SNR), differences in power in the band 0.01–0.25 Hz between the missing hand's ROI and the intact hand's ROI in amputees and controls were also examined. No significant interaction was identified between hemisphere and group ($F_{(1,37)} = 2.61$, $p = 0.115$). This suggests that changes in SNR do not underlie the changes in connectivity documented here (see also Table S2).

To confirm that the observed association between intra-network decoupling and inter-network coupling was specifically associated with amputation, this phenomena was also assessed in the control group and the control ROI. This correlation was not observed in the controls ($\rho_{(19)}$ for controls $= 0.274$, $p = 0.274$; Fisher's r-to-z controls vs amputees $= -2.33$, $p = 0.01$), or in the ipsilateral hand area in amputees ($\rho_{(16)} = -0.15$; $p = 0.55$). These control tests support the notion that the observed inter-network plasticity was uniquely associated with the amputees' missing hand cortex. See the Supplementary section for further analysis addressing the potential confound of network asymmetries.

Specificity of the DMN

The results described above provide information about the coupling of the missing hand cortex with the entire DMN, based on an averaged signal. To further interrogate the relationship between the missing hand cortex and the DMN we performed a seed-based analysis. This approach is based on calculating the temporal synchronicity in resting fMRI time course between the missing hand cortex ('seed') and all other voxels in the brain (Biswal et al., 1995). Unlike the dual regression approach described above, which provides information about the unique contribution of a specific network beyond partial contributions of other networks, the seed signal likely contains many overlapping individual signal components that we cannot dissociate. Nevertheless, it provides an opportunity to validate and extend the main results obtained using the dual regression, as it allows us to identify which specific loci might underlie the observed increased coupling between the missing hand ROI and the DMN.

When comparing connectivity maps between amputees and controls, significantly greater connectivity was found for amputees in the dorsomedial prefrontal cortex extending to the anterior cingulate cortex, and posterior cingulate cortex bilaterally, as well as the dorsolateral frontal cortex and the angular gyrus ipsilateral to the seed region (Fig. 3, Table 2). These seed-based clusters partially overlapped with the DMN component identified in the ICA, as shown in Fig. 2A. When performing the opposite contrast (controls > amputees), no significant clusters were found.

To test which of the 8 canonical resting-state networks (identified using the ICA, see above) was most similar to the seed-based clusters shown in Fig. 3 (i.e. the results of the group contrast map for the missing hand seed analysis, hereafter seed-based map), we estimated the spatial overlap between them using whole-brain cross correlation. We used a 'winner takes all' approach to identify which of the 8 canonical networks represents best the (unthresholded) seed-based map. No further statistical inferences were made based on the spatial r-values, due to concerns of data over-fitting. The DMN showed the highest overlap with the seed-based map ($r_{(212,287)} = 0.28$), suggesting greatest overlap between the seed-based map and the DMN.

The seed-based map reported in Fig. 3 could be driven by a net reduction in connectivity in the control group, or by increased connectivity between the amputees' missing hand ROI and the highlighted areas. To investigate the direction of connectivity changes underlying the seed-based maps, we calculated the level of connectivity between the voxels underlying the seed-based map and the missing hand ROI in individual participants (see Methods). While the control group showed on average no connectivity between the hand seed and the seed-based map (mean ± s.e.m. $= 0.01 \pm 0.01$; $t_{(20)} = 1$, $p = 0.33$ against zero), the amputee group showed significant positive betas (mean ± s.e.m. $= 0.11 \pm 0.01$; $t_{(17)} = 9.5$, $p < 0.001$ against zero). This analysis shows us that functional connectivity between the missing hand seed ROI and the seed-based map was positive in the amputees. This increased coupling between the missing hand ROI and the set of regions shown in Fig. 3 in the amputees but not the controls is compatible with that observed in the DMN dual regression analysis (i.e. increased connectivity between the DMN and the missing hand ROI in amputees but not controls, see Fig. 2C).

Finally, to determine whether the increased connectivity of the cortical territory of the missing hand is specific to the DMN, we repeated the same analysis as described in Fig. 2 with two control ICA components. First, we examined a component encompassing the insula and operculum (as shown in Fig. S1A), which have been shown to alter in connectivity in chronic pain patients (Baliki et al., 2014; Kim et al., 2013; Napadow et al., 2010). We didn't identify any significant group differences in connectivity between the missing hand cortex and the insular-operculum network ($t_{(37)} = -0.722$, $p = 0.475$; Fig. S1B). However, we did find a significant positive correlation between strength of coupling between the hand area and the sensorimotor network in amputees, and strength of coupling between the hand area and the insula-operculum network ($\rho_{(16)} = -0.547$, $p = 0.019$; Fig. S1C). This indicates that individuals showing stronger connectivity between the missing hand cortex and its network of origin also show greater coupling with the insula and/or operculum. This contrasts with the DMN, for which stronger coupling between the missing hand cortex and sensorimotor cortex was associated with weaker coupling between missing hand cortex and DMN.

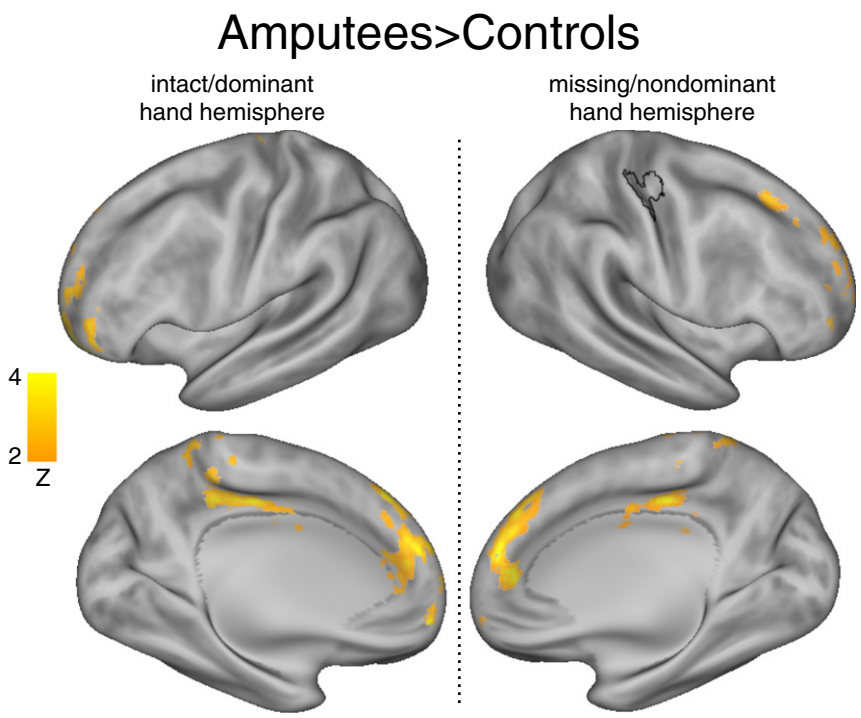

Fig. 3. Areas showing increased connectivity with the missing hand cortex in amputees, based on a seed-analysis. Whole brain contrast between amputees and controls of connectivity maps with the missing hand seed ROI. Significant clusters are projected on an averaged cortical surface. The black contours visible on the cortical surface (top right) denote the borders of the missing hand cortex ($Z > 7$). Intact/dominant hand hemisphere is the hemisphere contralateral to the intact hand in amputees and dominant hand in controls. Missing/nondominant hand hemisphere is the hemisphere contralateral to the missing hand in amputees and the dominant hand in controls.

We also investigated the component corresponding to the executive control network (Pievani et al., 2014; Seeley et al., 2007). This component encompassed brain regions including the dorsolateral prefrontal cortex, medial frontal cortex, posterior cingulate cortex, supramarginal gyrus and precuneus cortex, as shown in Fig. S2A. It was chosen since it showed the 2nd highest overlap with the unthresholded map of areas with stronger connectivity to the missing hand area in amputees versus controls (seed-based map in Fig. 3; $r_{(212,287)} = 0.20$). The executive control network was found to not be connected to the sensorimotor hand area, both in controls (nondominant hand ROI, mean beta ± s.e.m. $= -0.02 \pm 0.25$) and in amputees (missing hand ROI, mean beta ± s.e.m. $= 0.04 \pm 0.23$), resulting in a non-significant group difference ($p > 0.85$). Furthermore, no significant correlation was identified in amputees between connectivity of the hand ROI to the executive control network and to the sensorimotor network ($\rho_{(16)} = -0.253$; $p = 0.311$). These results further confirm that inter-network plasticity of the sensorimotor network is specific to the DMN.

Table 2
Summary of functional location, Z values and peak voxel location (MNI coordinates) for areas showing increased connectivity with the missing hand cortex in amputees, compared with controls, as shown in Fig. 3.

	Z	x	y	z
Dorsomedial prefrontal cortex (missing-ipsilateral hemisphere)	3.68	−4	58	32
Dorsomedial prefrontal cortex (missing-contralateral cortex)	3.54	2	40	40
Anterior cingulate cortex (missing-contralateral cortex)	3.77	6	48	22
Dorsolateral frontal cortex (missing-contralateral cortex)	3.34	22	18	44
Posterior cingulate cortex (missing-contralateral cortex)	3.62	4	−24	38
Angular gyrus[a] (missing-contralateral cortex)	2.74	44	−54	56

Missing-contralateral refers to the hemisphere contralateral to the missing hand (amputees) or nondominant hand (controls). Missing-ipsilateral refers to the hemisphere ipsilateral to the missing hand (amputees) or nondominant hand (controls).

[a] The cluster on the angular gyrus is not visible on the inflated map as it was located very close to the brain edge.

Network-level plasticity and inter-individual clinical variability

We next examined whether inter-individual changes in connectivity strength between the missing hand territory and the two networks could be explained by clinical variables relating to the amputation. In particular, we were interested in identifying the potential roles of time since amputation, phantom sensations and pain in determining the dissociation from the sensorimotor system and the association to the DMN. Table S2 provides information on bivariate Spearman correlations between 8 different clinical variables (as well as spectral power within the missing hand ROI) and functional connectivity to each of the two networks of interest, as well as the insular-operculum network. We found a significant negative correlation between connectivity strength (between the missing hand ROI and the sensorimotor network) and time since amputation: individuals amputated for longer periods also showed reduced coupling between the missing hand cortex and the sensorimotor network ($\rho_{(16)} = -0.72$, $p = 0.001$, adjusted $p = 0.008$; Fig. 1D). No significant bivariate correlations (after correction for multiple comparisons) were found for the DMN (see Supplementary section for a discussion about the potential role of ongoing phantom pain in driving connectivity with the DMN) or the insular-operculum network.

To determine how these clinical variables may interact with each other in order to drive changes in functional connectivity in the amputees, we also used a backward elimination linear regression (see Methods). For the sensorimotor network, the final model included time since amputation as a single independent variable ($R^2 = 0.41$, $F_{(1,16)} = 11.25$, $p = .004$.; adjusted $R^2 = 0.38$). For the DMN, the most parsimonious model relied on functional connectivity between the sensorimotor network and the missing hand cortex, and phantom pain magnitude (which takes into account both phantom pain intensity and frequency, reflecting a chronic measurement of phantom pain, see Makin et al., 2013b) as independent variables ($R^2 = 0.34$, $F_{(2,15)} = 3.89$, $p = 0.044$.; adjusted $R^2 = 0.254$). These results suggest that the

main driver for decoupling from the sensorimotor cortex may be time since amputation, whereas coupling with the DMN depends on both dissociation from the network of origin and increased phantom pain, although the contribution of phantom pain to the final model was only marginally significant ($t = 2.00$, $p = 0.064$), and should therefore be interpreted with caution.

Discussion

The use of resting-state functional connectivity enabled us to examine the interplay between the missing hand cortex and multiple networks with dissociated functional roles across the entire brain, simultaneously. Our results show large-scale reorganisation of the missing hand's cortex beyond the sensorimotor system. Specifically, over the course of years, the missing hand cortex gradually becomes functionally decoupled from the sensorimotor network (Fig. 1). This process is associated with increasing functional coupling with medial prefrontal and parietal areas, best characterised as the default mode network (DMN) (Figs. 2 and 3), from which the primary sensorimotor cortex is normally uncoupled (Hale et al., 2010) (also shown in controls in Fig. 2C). Our approach therefore allowed us to identify large-scale changes in the brain following hand amputation, beyond the scope that has been studied before using electrophysiology, or task-based functional imaging.

What processes might be driving the observed reduction in functional connectivity between the missing hand cortex and its network of origin? Arm amputation results in immediate deprivation of major inputs and outputs to the primary somatosensory and motor cortices. This will lead to unmasking of silenced inputs, as well as remodelling of dendritic and axonal sprouting, both locally (e.g. within the synaptic gap), and more globally (Barnes and Finnerty, 2010). Reduced inputs could therefore potentially trigger some of the observed decoupling with the sensorimotor network, at least at a short time-scale (Merabet et al., 2008) (see Pawela et al., 2010 for related findings in rats). However, given that the decoupling increased over the years, other mechanisms should be considered. Second, we have previously shown that the missing hand cortex supports adaptive behaviour of the intact hand in amputees (Makin et al., 2013a). This rebalancing of inputs might affect overall signal fluctuations as observed during rest, leading to changes in net functional connectivity. Indeed, we recently showed that levels of functional connectivity between the two hand areas in individuals with congenital hand loss scale with compensatory every-day usage of their residual arm during bimanual tasks (Hahamy et al., 2015). However, given that the level of connectivity studied here is determined based on a global (averaged) signal of the sensorimotor system, and given that at least some of the adaptive changes might be associated with up-regulation of neighbouring or homologous sensorimotor inputs, adaptive changes might not necessarily drive decoupling from the sensorimotor network (see also Yu et al., 2013). Finally, arm amputation is commonly accompanied by maintained sensation of the missing hand (phantom sensations). We have previously reported that chronic phantom pain is associated with preserved structure and function in the missing hand cortex (Makin et al., 2013b). This is consistent with current research demonstrating that both painful and non-painful phantom sensations are driven by ectopic firing from the injured primary afferents (Vaso et al., 2014). This increased peripheral input will be reflected in a change of the net signal specifically within the missing hand's cortex, therefore resulting in decoupling of this region from the rest of the sensorimotor network. It is likely that sensory deprivation, adaptive plasticity and increased aberrant input all contribute to the observed reduction in coupling between the missing hand cortex and the sensorimotor network.

As indicated by our backward regression model, the observed decrease in sensorimotor coupling may be a primary driver of the increased association of the missing hand's territory with the DMN. Given that phantom sensations are isolated from other sensory experiences relevant for motor control of the hand, and given that phantom sensations are largely prevalent in amputees, the phenomenon of increased peripheral aberrant inputs might potentially contribute not only to the observed detachment from the sensorimotor network, but also the related association with the DMN. Indeed, the analysis approach taken here (dual regression) is designed to identify network specificity, and as such the increased connectivity of the missing hand cortex was specific to the DMN (see Fig. 3 and Figs. S1–S2 for complementary results). We therefore suggest that the coupling with the DMN was not merely a passive consequence of decoupling from the sensorimotor network. We had originally predicted increased coupling between the missing hand cortex and the DMN because of the involvement of DMN regions in internal modes, and the prevalence of phantom sensations in amputees. Moreover, greater connectivity with and within the DMN has previously been linked with chronic pain in other pain conditions (Baliki et al., 2008, 2014; Bolwerk et al., 2013; Napadow et al., 2010). As we did not identify a clear statistical relationship between increased coupling with the DMN and chronic pain (as well as a range of other phantom sensations, Table S2), we cannot confirm our prediction. However, our backward regression analysis suggests that chronic phantom pain may support the emerging association with the DMN. Further research is required in order to test these predictions directly.

Alternatively, it is also possible that the selective coupling of the missing hand cortex with the DMN was further facilitated by the resting state set-up used here (i.e. participants are not engaged with external stimuli, but are asked to keep awake) — a context which may particularly activate the DMN, as participants engage in internal modes of cognition (Buckner et al., 2013). Due to the decoupling from the sensorimotor network, the missing hand cortex in amputees may be available to couple with a range of networks, and may show preferential functional connectivity with whichever networks are currently most active. Given that activation in the DMN is selectively increased during rest, this may result in apparently selective coupling with the DMN, but in fact be driven by context.

To conclude, we demonstrate that despite the apparently preserved representation of the missing hand, arm amputation cascades cortical reorganisation at multiple scales, within and beyond the scope of the sensorimotor network. Over the past two decades, local remapping has been considered a promising target for neurorehabilitation (Ramachandran and Altschuler, 2009), as it has been thought to drive chronic pain (Flor et al., 1995; Gustin et al., 2012). Yet, how local remapping can trigger such a complex perceptual experience remains unclear. By revealing a relationship between sensorimotor plasticity and coupling with the DMN, our results shed new light on this important issue. Further study of the adaptive and maladaptive behavioural correlates of network-level reorganisation may therefore bear clinical potential.

Acknowledgments

Supporting bodies: TRM: Royal Society (Newton International Fellowship), European Commission (Marie Curie Intra-European Fellowship) and Sir Henry Dale Fellowship jointly funded by the Wellcome Trust and the Royal Society (grant no. 104128/Z/14/Z). HJB: People Programme (Marie Curie Actions) FP7/2007-2013 under the Intra-European Fellowship and REA grant agreement no. PITN-GA-2011-290011. HJB and IT: Wellcome Trust, the National Institute for Health Research (NIHR) Oxford Biomedical Research Centre based at Oxford University Hospitals NHS Trust and University of Oxford. NF: HDH Wills 1965 Charitable Trust. We thank our participants and Opcare for their help in carrying the study.

Appendix A. Supplementary data

Supplementary data to this article can be found online at http://dx.doi.org/10.1016/j.neuroimage.2015.02.067.

References

Baliki, M.N., Geha, P.Y., Apkarian, A.V., Chialvo, D.R., 2008. Beyond feeling: chronic pain hurts the brain, disrupting the default-mode network dynamics. J. Neurosci. 28, 1398–1403. http://dx.doi.org/10.1523/JNEUROSCI. 4123-07.2008.

Baliki, M.N., Mansour, A.R., Baria, A.T., Apkarian, A.V., 2014. Functional reorganization of the default mode network across chronic pain conditions. PLoS ONE 9, e106133. http://dx.doi.org/10.1371/journal.pone.0106133.

Barnes, S.J., Finnerty, G.T., 2010. Sensory experience and cortical rewiring. Neuroscientist 16, 186–198. http://dx.doi.org/10.1177/1073858409343961.

Beckmann, C.F., DeLuca, M., Devlin, J.T., Smith, S.M., 2005. Investigations into resting-state connectivity using independent component analysis. Philos. Trans. R. Soc. Lond. B Biol. Sci. 360, 1001–1013. http://dx.doi.org/10.1098/rstb.2005.1634.

Biswal, B., Yetkin, F.Z., Haughton, V.M., Hyde, J.S., 1995. Functional connectivity in the motor cortex of resting human brain using echo-planar MRI. Magn. Reson. Med. 34, 537–541.

Bogdanov, S., Smith, J., Frey, S.H., 2012. Former hand territory activity increases after amputation during intact hand movements, but is unaffected by illusory visual feedback. Neurorehabil. Neural Repair http://dx.doi.org/10.1177/1545968311429687.

Bolwerk, A., Seifert, F., Maihöfner, C., 2013. Altered resting-state functional connectivity in complex regional pain syndrome. J. Pain 14, 1107–1115. http://dx.doi.org/10.1016/j.jpain.2013.04.007 (e8).

Buckner, R.L., Andrews-Hanna, J.R., Schacter, D.L., 2008. The brain's default network: anatomy, function, and relevance to disease. Ann. N. Y. Acad. Sci. 1124, 1–38. http://dx.doi.org/10.1196/annals.1440.011.

Buckner, R.L., Krienen, F.M., Yeo, B.T.T., 2013. Buckner opportunities and limitations of intrinsic functional connectivity MRI. NatNeurosci0613. Nat. Neurosci. 16, 832–837. http://dx.doi.org/10.1038/nn.3423.

Collignon, O., Dormal, G., Albouy, G., Vandewalle, G., Voss, P., Phillips, C., Lepore, F., 2013. Impact of blindness onset on the functional organization and the connectivity of the occipital cortex. Brain 136, 2769–2783. http://dx.doi.org/10.1093/brain/awt176.

Diers, M., Christmann, C., Koeppe, C., Ruf, M., Flor, H., 2010. Mirrored, imagined and executed movements differentially activate sensorimotor cortex in amputees with and without phantom limb pain. Pain 149, 296–304. http://dx.doi.org/10.1016/j.pain.2010.02.020.

Douaud, G., Filippini, N., Knight, S., Talbot, K., Turner, M.R., 2011. Integration of structural and functional magnetic resonance imaging in amyotrophic lateral sclerosis. Brain 134, 3470–3479. http://dx.doi.org/10.1093/brain/awr279.

Draganski, B., Moser, T., Lummel, N., Gänssbauer, S., Bogdahn, U., Haas, F., May, A., 2006. Decrease of thalamic gray matter following limb amputation. NeuroImage 31, 951–957. http://dx.doi.org/10.1016/j.neuroimage.2006.01.018.

Filippini, N., MacIntosh, B.J., Hough, M.G., Goodwin, G.M., Frisoni, G.B., Smith, S.M., Matthews, P.M., Beckmann, C.F., Mackay, C.E., 2009. Distinct patterns of brain activity in young carriers of the APOE-epsilon4 allele. Proc. Natl. Acad. Sci. U. S. A. 106, 7209–7214. http://dx.doi.org/10.1073/pnas.0811879106.

Filippini, N., Nickerson, L.D., Beckmann, C.F., Ebmeier, K.P., Frisoni, G.B., Matthews, P.M., Smith, S.M., Mackay, C.E., 2012. Age-related adaptations of brain function during a memory task are also present at rest. NeuroImage 59, 3821–3828. http://dx.doi.org/10.1016/j.neuroimage.2011.11.063.

Flor, H., Elbert, T., Knecht, S., Wienbruch, C., Pantev, C., Birbaumer, N., Larbig, W., Taub, E., 1995. Phantom-limb pain as a perceptual correlate of cortical reorganization following arm amputation. Nature 375, 482–484. http://dx.doi.org/10.1038/375482a0.

Flor, H., Nikolajsen, L., Staehelin Jensen, T., 2006. Phantom limb pain: a case of maladaptive CNS plasticity? Nat. Rev. Neurosci. 7, 873–881. http://dx.doi.org/10.1038/nrn1991.

Florence, S.L., Taub, H.B., Kaas, J.H., 1998. Large-scale sprouting of cortical connections after peripheral injury in adult macaque monkeys. Science 282, 1117–1121.

Foell, J., Bekrater-Bodmann, R., Diers, M., Flor, H., 2013. Mirror therapy for phantom limb pain: brain changes and the role of body representation. EJP http://dx.doi.org/10.1002/j.1532-2149.2013.00433.x (n/a–n/a).

Friston, K.J., Frith, C.D., Liddle, P.F., Frackowiak, R.S., 1993. Functional connectivity: the principal-component analysis of large (PET) data sets. J. Cereb. Blood Flow Metab. 13, 5–14. http://dx.doi.org/10.1038/jcbfm.1993.4.

Greicius, M.D., Krasnow, B., Reiss, A.L., Menon, V., 2003. Functional connectivity in the resting brain: a network analysis of the default mode hypothesis. Proc. Natl. Acad. Sci. U. S. A. 100, 253–258. http://dx.doi.org/10.1073/pnas.0135058100.

Greve, D.N., Fischl, B., 2009. Accurate and robust brain image alignment using boundary-based registration. NeuroImage 48, 63–72. http://dx.doi.org/10.1016/j.neuroimage.2009.06.060.

Gustin, S.M., Peck, C.C., Cheney, L.B., Macey, P.M., Murray, G.M., Henderson, L.A., 2012. Pain and plasticity: is chronic pain always associated with somatosensory cortex activity and reorganization? J. Neurosci. 32, 14874–14884. http://dx.doi.org/10.1523/JNEUROSCI. 1733-12.2012.

Hahamy, A., Sotiropoulos, S.N., Henderson Slater, D., Malach, R., Johansen-Berg, H., Makin, T.R., 2015. Normalisation of brain connectivity through compensatory behaviour, despite congenital hand absence. eLife 4. http://dx.doi.org/10.7554/eLife.04605.

Hale, J.R., Brookes, M.J., Hall, E.L., Zumer, J.M., Stevenson, C.M., Francis, S.T., Morris, P.G., 2010. Comparison of functional connectivity in default mode and sensorimotor networks at 3 and 7 T. MAGMA 23, 339–349. http://dx.doi.org/10.1007/s10334-010-0220-0.

Jain, N., Qi, H.-X., Collins, C.E., Kaas, J.H., 2008. Large-scale reorganization in the somatosensory cortex and thalamus after sensory loss in macaque monkeys. J. Neurosci. 28, 11042–11060. http://dx.doi.org/10.1523/JNEUROSCI. 2334-08.2008.

Kim, J.-Y., Kim, S.-H., Seo, J., Kim, S.-H., Han, S.W., Nam, E.J., Kim, S.-K., Lee, H.J., Lee, S.-J., Kim, Y.-T., Chang, Y., 2013. Increased power spectral density in resting-state pain-related brain networks in fibromyalgia. Pain 154, 1792–1797. http://dx.doi.org/10.1016/j.pain.2013.05.040.

Lotze, M., Flor, H., Grodd, W., Larbig, W., Birbaumer, N., 2001. Phantom movements and pain. An fMRI study in upper limb amputees. Brain 124, 2268–2277.

MacIver, K., Lloyd, D.M., Kelly, S., Roberts, N., Nurmikko, T., 2008. Phantom limb pain, cortical reorganization and the therapeutic effect of mental imagery. Brain 131, 2181–2191. http://dx.doi.org/10.1093/brain/awn124.

Makin, T.R., Wilf, M., Schwartz, I., Zohary, E., 2010. Amputees "neglect" the space near their missing hand. Psychol. Sci. 21, 55–57. http://dx.doi.org/10.1177/0956797609354739.

Makin, T.R., Cramer, A.O., Scholz, J., Hahamy, A., Henderson Slater, D., Tracey, I., Johansen-Berg, H., 2013a. Deprivation-related and use-dependent plasticity go hand in hand. eLife 2. http://dx.doi.org/10.7554/eLife.01273.

Makin, T.R., Scholz, J., Filippini, N., Henderson Slater, D., Tracey, I., Johansen-Berg, H., 2013b. Phantom pain is associated with preserved structure and function in the former hand area. Nat. Commun. 4, 1570. http://dx.doi.org/10.1038/ncomms2571.

Makin, T.R., Brozzoli, C., Cardinali, L., Holmes, N.P., Farnè, A., 2014. Left or right? Rapid visuomotor coding of hand laterality during motor decisions. CORTEX 64C, 289–292. http://dx.doi.org/10.1016/j.cortex.2014.12.004.

Markov, N.T., Ercsey-Ravasz, M., Van Essen, D.C., Knoblauch, K., Toroczkai, Z., Kennedy, H., 2013. Cortical high-density counterstream architectures. Science 342, 1238406. http://dx.doi.org/10.1126/science.1238406.

Merabet, L.B., Hamilton, R., Schlaug, G., Swisher, J.D., Kiriakopoulos, E.T., Pitskel, N.B., Kauffman, T., Pascual-Leone, A., 2008. Rapid and reversible recruitment of early visual cortex for touch. PLoS ONE 3, e3046. http://dx.doi.org/10.1371/journal.pone.0003046.

Napadow, V., LaCount, L., Park, K., As-Sanie, S., Clauw, D.J., Harris, R.E., 2010. Intrinsic brain connectivity in fibromyalgia is associated with chronic pain intensity. Arthritis Rheum. 62, 2545–2555. http://dx.doi.org/10.1002/art.27497.

Niazy, R.K., Xie, J., Miller, K., Beckmann, C.F., Smith, S.M., 2011. Spectral characteristics of resting state networks. Prog. Brain Res. 193, 259–276. http://dx.doi.org/10.1016/B978-0-444-53839-0.00017-X.

Nieuwenhuis, S., Forstmann, B.U., Wagenmakers, E.-J., 2011. Erroneous analyses of interactions in neuroscience: a problem of significance. Nat. Neurosci. 14, 1105–1107. http://dx.doi.org/10.1038/nn.2886.

Park, C.-H., Chang, W.H., Ohn, S.H., Kim, S.T., Bang, O.Y., Pascual-Leone, A., Kim, Y.-H., 2011. Longitudinal changes of resting-state functional connectivity during motor recovery after stroke. Stroke 42, 1357–1362. http://dx.doi.org/10.1161/STROKEAHA.110.596155.

Pawela, C.P., Biswal, B.B., Hudetz, A.G., Li, R., Jones, S.R., Cho, Y.R., Matloub, H.S., Hyde, J.S., 2010. Interhemispheric neuroplasticity following limb deafferentation detected by resting-state functional connectivity magnetic resonance imaging (fcMRI) and functional magnetic resonance imaging (fMRI). NeuroImage 49, 2467–2478. http://dx.doi.org/10.1016/j.neuroimage.2009.09.054.

Pievani, M., Filippini, N., van den Heuvel, M.P., Cappa, S.F., Frisoni, G.B., 2014. Brain connectivity in neurodegenerative diseases—from phenotype to proteinopathy. Nat. Rev. Neurol. 10, 620–633. http://dx.doi.org/10.1038/nrneurol.2014.178.

Pons, T.P., Garraghty, P.E., Ommaya, A.K., Kaas, J.H., Taub, E., Mishkin, M., 1991. Massive cortical reorganization after sensory deafferentation in adult macaques. Science 252, 1857–1860.

Raffin, E., Mattout, J., Reilly, K.T., Giraux, P., 2012. Disentangling motor execution from motor imagery with the phantom limb. Brain 135, 582–595. http://dx.doi.org/10.1093/brain/awr337.

Raichle, M.E., MacLeod, A.M., Snyder, A.Z., Powers, W.J., Gusnard, D.A., Shulman, G.L., 2001. A default mode of brain function. Proc. Natl. Acad. Sci. U. S. A. 98, 676–682.

Ramachandran, V.S., Altschuler, E.L., 2009. The use of visual feedback, in particular mirror visual feedback, in restoring brain function. Brain 132, 1693–1710. http://dx.doi.org/10.1093/brain/awp135.

Rizzolatti, G., Matelli, M., 2003. Two different streams form the dorsal visual system: anatomy and functions. Exp. Brain Res. 153, 146–157. http://dx.doi.org/10.1007/s00221-003-1588-0.

Rocca, M.A., Valsasina, P., Fazio, R., Previtali, S.C., Messina, R., Falini, A., Comi, G., Filippi, M., 2014. Brain connectivity abnormalities extend beyond the sensorimotor network in peripheral neuropathy. Hum. Brain Mapp. 35, 513–526. http://dx.doi.org/10.1002/hbm.22198.

Seeley, W.W., Menon, V., Schatzberg, A.F., Keller, J., Glover, G.H., Kenna, H., Reiss, A.L., Greicius, M.D., 2007. Dissociable intrinsic connectivity networks for salience processing and executive control. J. Neurosci. 27, 2349–2356. http://dx.doi.org/10.1523/JNEUROSCI. 5587-06.2007.

Smith, S.M., Fox, P.T., Miller, K.L., Glahn, D.C., Fox, P.M., Mackay, C.E., Filippini, N., Watkins, K.E., Toro, R., Laird, A.R., Beckmann, C.F., 2009. Correspondence of the brain's functional architecture during activation and rest. Proc. Natl. Acad. Sci. U. S. A. 106, 13040–13045. http://dx.doi.org/10.1073/pnas.0905267106.

Smith, S.M., Miller, K.L., Moeller, S., Xu, J., Auerbach, E.J., Woolrich, M.W., Beckmann, C.F., Jenkinson, M., Andersson, J., Glasser, M.F., Van Essen, D.C., Feinberg, D.A., Yacoub, E.S., Uğurbil, K., 2012. Temporally-independent functional modes of spontaneous brain activity. Proc. Natl. Acad. Sci. U. S. A. 109, 3131–3136. http://dx.doi.org/10.1073/pnas.1121329109.

Vaso, A., Adahan, H.-M., Gjika, A., Zahaj, S., Zhurda, T., Vyshka, G., Devor, M., 2014. Peripheral nervous system origin of phantom limb pain. Pain http://dx.doi.org/10.1016/j.pain.2014.04.018.

Weeks, S.R., Anderson-Barnes, V.C., Tsao, J.W., 2010. Phantom limb pain: theories and therapies. Neurologist 16, 277–286. http://dx.doi.org/10.1097/NRL.0b013e3181edf128.

Wilf, M., Holmes, N.P., Schwartz, I., Makin, T.R., 2013. Dissociating between object affordances and spatial compatibility effects using early response components. Front. Psychol. 4, 591. http://dx.doi.org/10.3389/fpsyg.2013.00591.

Yeo, B.T.T., Krienen, F.M., Sepulcre, J., Sabuncu, M.R., Lashkari, D., Hollinshead, M., Roffman, J.L., Smoller, J.W., Zöllei, L., Polimeni, J.R., Fischl, B., Liu, H., Buckner, R.L., 2011. The organization of the human cerebral cortex estimated by intrinsic functional connectivity. J. Neurophysiol. 106, 1125–1165. http://dx.doi.org/10.1152/jn.00338.2011.

Yu, X.J., He, H.J., Zhang, Q.W., Zhao, F., Zee, C.S., Zhang, S., Gong, X.Y., 2013. Somatotopic reorganization of hand representation in bilateral arm amputees with or without special foot movement skill. Brain Res. http://dx.doi.org/10.1016/j.brainres.2013.12.025.